

## **Response to reviewer #1**

Dentith et al. describe the implementation of radiocarbon ( $^{14}\text{C}$ , or  $\Delta^{14}\text{C}$  when considering the normalized and fractionation-corrected  $^{14}\text{C}/^{12}\text{C}$  ratio) into the ocean component of the FAMOUS atmosphere-ocean GCM and present two  $^{14}\text{C}$  simulations, one spin-up simulation with constant pre-industrial boundary conditions plus a “historical” simulation forced with transient values of atmospheric  $\text{CO}_2$  and  $\Delta^{14}\text{C}$  for 1765–2000 CE. The simulation results are compared with water column measurements available for the 1950s and the 1990s, and with  $^{14}\text{C}$  records from bivalves and deep-water corals spanning the period 1880–2000 CE. The model results are at least qualitatively in line with observations. FAMOUS simulates radiocarbon in two ways. The “abiotic” approach only considers uptake, transport and radioactive decay of normalized  $^{14}\text{C}/^{12}\text{C}$ . The “biotic” approach also considers isotopic fractionation due to air-sea gas exchange and the isotopic imprint of the biological pump. Comparing both approaches, Dentith et al. find that the “biotic” approach results in slightly elevated  $^{14}\text{C}/^{12}\text{C}$  ratios in the deep sea (by about 20 ‰ in terms of  $\Delta^{14}\text{C}$ ). This result corroborates early findings stating that biological effects on  $^{14}\text{C}/^{12}\text{C}$  are much smaller (<10 %) than the effects of transport and radioactive decay (Fiadeiro, 1982). In addition, Dentith et al. compare simulated  $^{14}\text{C}$  water ages with “true” water ages according to an idealized age tracer. It turns out that for large parts of the oceans, a purely kinematic interpretation of  $^{14}\text{C}/^{12}\text{C}$  ages can lead to erroneous conclusions.

The paper is well written, the presentation of the results is mostly clear, and the literature is comprehensive. It may be published if the following issues are amended:

*We would like to thank reviewer #1 for their feedback on our manuscript. We have considered all of the comments carefully and addressed them in turn below, with our responses in blue-italics.*

**Major issue:** As described in Section 2.3.2, the model setup does not allow for meridional variability of atmospheric  $\Delta^{14}\text{C}$ . Therefore, the historical simulation misses the strong interhemispheric  $\Delta^{14}\text{C}$  gradient in the atmosphere of up to 400 ‰ (e.g., Fig. 1 in the manuscript) due to nuclear weapons testing. As a consequence, the model may underestimate the actual spatiotemporal  $^{14}\text{C}$  gradients in the ocean since the late 1950s. This shortcoming may distort the evolution of bomb  $^{14}\text{C}$  transients discussed in Section 3.3. It may also lead to biased post-bomb  $^{14}\text{C}$  distributions in subsurface and deeper waters which are discussed in Section 3.2. I would strongly recommend repeating the historical simulation forced with hemispheric averages of atmospheric  $\Delta^{14}\text{C}$ . The implementation should not be too difficult (the model has to read in three files provided by OCMIP-2).

*Whilst we agree that prescribing multiple latitude bands for both atmospheric  $\text{CO}_2$  and  $\Delta^{14}\text{C}$  would allow the north-south gradient in fossil fuel emissions and the location of atmospheric nuclear weapons testing to be better represented, this would require substantial changes to the code because FAMOUS, as with all configurations of version 4.5 of the Unified Model, currently only allows a single atmospheric value to be prescribed per year (both spatially and temporally). This project is no longer being funded, therefore we are unable to make this change.*

*In the future, it is intended that the isotope-enabled model will primarily be used to study changes in ocean circulation and the marine carbon cycle in a palaeo context, for example, at the Last Glacial Maximum (21,000 years ago) and during the last deglaciation (21,000 to 11,000 years ago). On these timescales, the atmosphere can be considered to be globally well-mixed, therefore meridional variability would not be required.*

**Further issues and comments (P = page, L = line, SM = supplementary material):**

P 3, L 6: The value of the half-life should be consistent with the updated value of 5700 years promoted in the SM.

*Although this would be a minor revision to the code, re-running the simulations and repeating the analyses would be a significant amount of work for minimal gain, especially since this project is no longer being funded. As outlined in the Supplementary Material, we recommend that the revised half-life is used for future scientific applications of the isotope-enabled model (i.e. the next time that a 10,000 year spin-up simulation is conducted, the new half-life should be employed as standard). However, we do not feel that it is necessary to make this change for our current study because the outdated half-life ( $5730 \pm 40$  years) and revised half-life ( $5700 \pm 30$  years) have overlapping error ranges, and re-running the model and our analyses with the updated half-life would not significantly alter the simulated isotope distributions or our interpretations.*

*The general formula for exponential decay is:*

$$N_{(t)} = N_0 2^{-\frac{t}{t_{1/2}}}$$

*where  $N_{(t)}$  is the amount of substance remaining at time 't',  $N_0$  is the initial amount of the substance, and  $t_{1/2}$  is the half-life of the substance.*

*We can therefore calculate the error associated with using the outdated half-life. At the end of the spin-up simulation (i.e. when  $t = 10,000$ ), the amount of  $^{14}\text{C}$  remaining ( $N_{10,000}$ ) using the outdated half-life of 5730 years is 0.298, whereas the amount remaining with the revised half-life of 5700 years is 0.296. This is the maximum error because the difference between the two half-lives is smaller for younger water parcels. For example,  $N_{1000}$  is 0.8855 using a half-life of 5730 years, and 0.8861 using a half-life of 5700 years.*

P 3, L 28: “Indian” should read “Indien”

*This typographical error will be corrected in the revised manuscript.*

P 4, L 28: The models MOM (Toggweiler et al., 1989), LOCH (Mouchet, 2013) and LOVEVLIM (e.g., Men viel et al. 2017) could be added to the list.

*Our intention was to provide illustrative examples of  $^{14}\text{C}$ -enabled models across a range of complexities as opposed to a complete list of all  $^{14}\text{C}$ -enabled models, but we are happy to add these additional examples in the revised manuscript.*

P 7, L 28:  $(660 / \text{Sc})^{**}-0.5$  should read  $(\text{Sc} / 660)^{**}-0.5$  (e.g., Orr et al. 2017, equation (12))

*This typographical error will be corrected in the revised manuscript.*

P 7, L 31: Missing reference (I guess it is Wanninkhof 1992)

*The reference (Wanninkhof, 1992) will be added in the revised manuscript.*

P 8, L 8 and P 22, L 27: I could not find the paper at GMDD. What is the current status of the manuscript?

*Technical journal requirements held up the progress of this manuscript, but it is now available in GMDD (<https://www.geosci-model-dev-discuss.net/gmd-2019-250/0>).*

P 8, L 12: 14 and 13 should be subscripts

*These typographical errors will be corrected in the revised manuscript.*

P 8, L 22: “ $\delta^{13}\text{C}$  is close to zero”: this is the only case for DIC but not for phytoplankton

*We will amend the text to “ $\delta^{13}\text{C}_{\text{DIC}}$  is close to zero” to avoid confusion.*

P 9, L 10: This is not correct, Stuiver and Pollach (1977) employ 5568 years.

*Stuiver and Polach (1977) is the reference for the equation:*

$$^{14}\text{C}_{\text{age}} = -\frac{\lambda}{\ln(2)} \times \ln \left( 1 + \frac{\Delta^{14}\text{C}}{1000} \right).$$

*However, we will add a sentence in the revised manuscript to clarify that we employ the Cambridge half-life ( $\lambda = 5730$  years), instead of the Libby half-life ( $\lambda = 5568$  years) used by Stuiver and Polach (1977).*

P 9, L 16: What about turbulent diffusion, where is it included?

*The ocean model has a tracer transport scheme that computes changes in tracer concentrations due to advection, diffusion, and mixing. We will make the following changes in the revised manuscript to clarify this:*

- *Section 2.2.5 will be renamed “Transport” instead of “Advection”*
- *“L” will be redefined as the “transport term, which includes advection (using flux-limited Quadratic Upstream Interpolation for Convective Kinematics, QUICK), diffusion, and mixing” instead of the “advection term”.*

P 9, L 26–28 and Figure S1: The OCMIP-2 steady state criterion is somewhat different, demanding that 98% of the ocean volume has a  $\Delta^{14}\text{C}$  drift of less than 0.001 ‰ per year (see also Aumont et al. 1998). The total  $^{14}\text{C}$  inventory may have stabilized while there might be still an ongoing internal redistribution of  $^{14}\text{C}$ . Have you checked this?

*We have verified that the internal redistribution of  $^{14}\text{C}$  at the end of the spin-up simulation is minimal.*

*We will revise the final sentence of Section 2.3.1 as follows:*

*“At the end of the spin-up simulation,  $\approx 99.8\%$  of the ocean has a  $\Delta^{14}\text{C}$  drift of less than 0.001 ‰  $\text{yr}^{-1}$  (equivalent to a change in  $^{14}\text{C}$  age of 8.27 years per millennia), satisfying the OCMIP-2 criterion for steady state (Orr et al., 2000).”*

P 13, L 5–6: “( . . . ) the simulated  $\Delta^{14}\text{C}$  gradient between the surface ocean and approximately 1000 m depth is shallower than observed ( . . . ). This is visible in all regions, except the Northern Hemisphere deep water formation region (NH\_DWF) and the North Pacific (NP) ( . . . ).” According to Figure 8 the opposite is true (indicating steeper simulated gradients everywhere except for NH\_DW and NP).

*In the near-surface ocean, the simulated change in  $\Delta^{14}\text{C}$  per unit depth is less than the observed change in all regions except the Northern Hemisphere deep water formation region and the North Pacific. We will correct this sentence in the revised manuscript, replacing “shallower” with “steeper”.*

P 13, L 23: “( . . . ) due to the sparsity of data.” You might wish to compare your results with post-bomb  $\Delta^{14}\text{C}$  (bottle) data provided by GLODAPv2 (<https://odv.awi.de/data/ocean/glodap-v22019-bottle-data/>).

*We have downloaded the GLODAPv2 Arctic Ocean data set from: <https://www.glodap.info/index.php/merged-and-adjusted-data-product/>. However, we have only been*

able to identify 64  $\Delta^{14}\text{C}$  data points from the 1990s. Specifically, these data are from six depth transects (with between 9 and 16 measurements at each location). They therefore provide insufficient resolution to contribute to our original spatial comparisons (Figures 4 and 6 in the original manuscript). However, a simple linear regression between these data and our simulated values at the corresponding grid cells in the model demonstrates that our simulated values are consistently lower than observed (Figure R1), which we propose is largely because FAMOUS has a cold temperature bias in the Arctic Ocean and around the coast of Greenland and Iceland that is linked with expanded annual sea ice in the Nordic and Labrador Seas (Dentith et al., 2019 - <https://link.springer.com/article/10.1007/s00382-018-4243-y>) – i.e. limiting the input of bomb  $^{14}\text{C}$  from the atmosphere to the ocean in this region. The observed depth transects extend between the surface ocean and approximately 3000 m depth, which approximately corresponds to the depths over which our simulated globally-averaged depth profile has a negative  $\Delta^{14}\text{C}$  bias relative to the observed profile (Figure 8 in the original manuscript). Thus, as well as our simulated global depth profile including the relatively low Arctic Ocean values that are missing from the original gridded GLODAP data set, our  $\Delta^{14}\text{C}$  values are lower than observed in this region, further compounding the negative bias. We will add a brief discussion of this analysis to the revised manuscript after these original sentences: “The masking in the GLODAP data set also contributes towards some of the offset between the model and the observations. For example, we include the relatively low Arctic Ocean values in our global, Northern Hemisphere deep water formation region (NH\_DWF) and Labrador Sea (LS) profiles, but these latitudes are masked out in GLODAP due to the sparsity of data (Figure 4a)”.

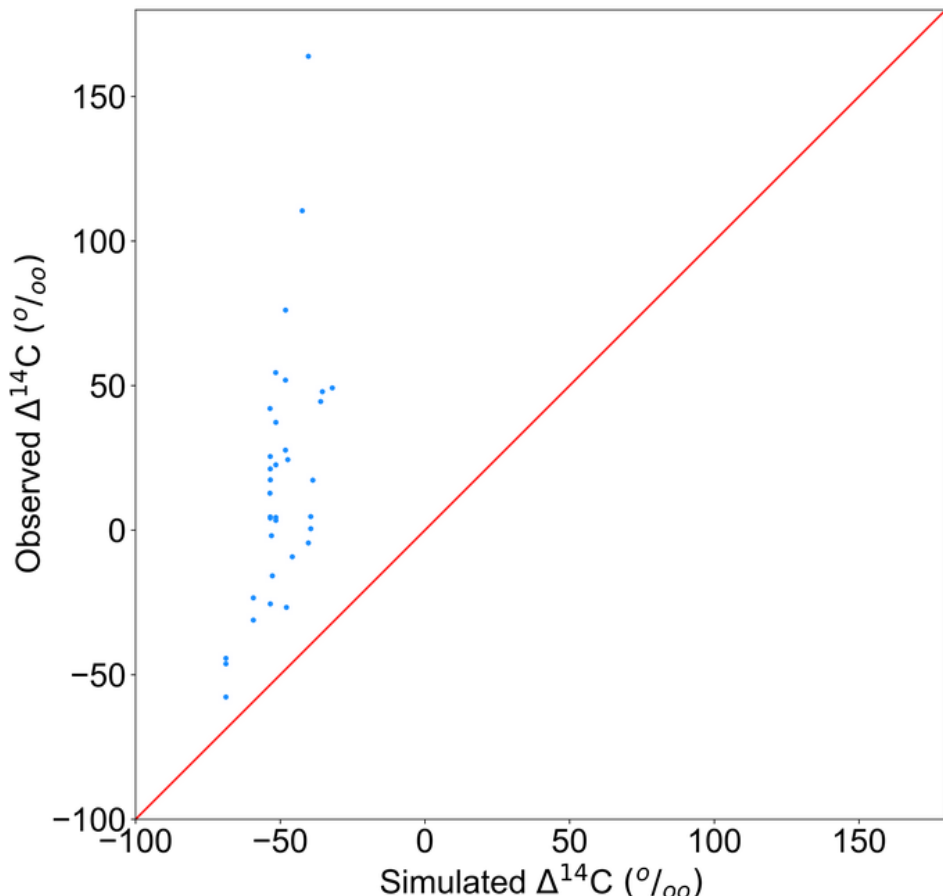


**Figure R1:** Simulated versus observed  $\Delta^{14}\text{C}$  values from the Arctic Ocean during the 1990s.

P 17, L 19: This is an interesting result supporting and quantifying the notion by Fiadeiro (1982) that  $^{14}\text{C}/^{12}\text{C}$  can roughly be regarded as radio-conservative tracer in the deep sea.

*We also thought this was an interesting result. However, in response to feedback from reviewer #2, we have decided to remove the abiotic-biotic comparison from our revised manuscript. This is because we have not yet found a way to present these results to both biogeochemical modellers and analytical biogeochemists without causing contention and confusion (see our response to reviewer #2 for further details). In the revised manuscript, we will remove all references to the pre-existing abiotic tracer, and instead will only present the comparison between biotic  $\Delta^{14}\text{C}$  and  $\Delta^{14}\text{C}$  observations, and the biotic  $^{14}\text{C}$  ages and the simulated water ages.*

P 18, L 1–6: The simulated  $^{14}\text{C}$  ages reflect local ageing, transport, biogeochemistry, and radioactive decay. On the other hand, the simulated ideal water ages only reflect local ageing and transport. As there is no radioactive decay of the age tracer, the age differences cannot be entirely explained with biogeochemical effects.

*Here, we consider the ageing of water and the radioactive decay of particles within a water mass to be equivalent processes – both are affected by the time since being reset at the surface. For example, because radioactive decay occurs at a known rate through time, this can be converted to an age since being reset at the surface. In Figure S6, we take into account that the water age is instantaneously reset at the surface, whereas the  $^{14}\text{C}$  has a reservoir age associated with isotopic equilibration rates, sea ice cover, and mixing, by normalising each depth profile relative to the surface ocean in each region; we therefore think it is a reasonable approximation to attribute the differences between the water ages and the  $^{14}\text{C}$  ages to ocean biogeochemistry.*

P 18, L 15–16: “(...) the water ages generally increase with depth because they are a simple function of advection.” I disagree, there may be considerable mixing leading to nonlinear ageing of water parcels. This is seen in many tracers records.

*In the revised manuscript, we will clarify that the water ages generally increase with depth because they are a function of the large-scale transport (i.e. in general, water parcels in the deep ocean have been out of contact with the atmosphere longer than water parcels at intermediate depths). We will also clarify that the increase in water age with depth is non-linear because of the mixing of water parcels of different ages.*

P 31, Figure 4 (b): I would prefer to see the differences between simulated and observed values, analogously to Figure 2.

*We will add a third subplot to Figure 4 to show the difference between the simulated and observed values, as below:*

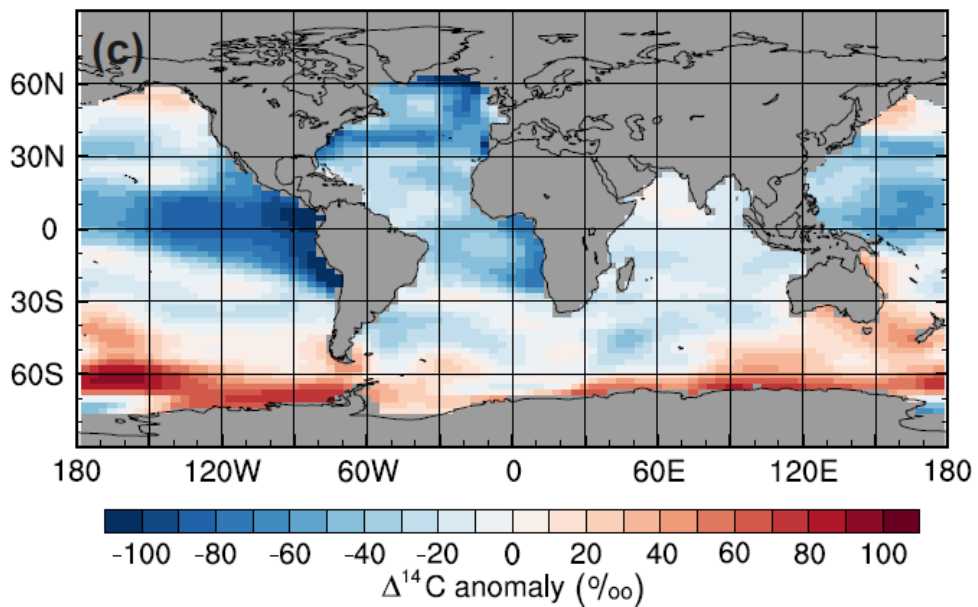


**Figure 4: (c)** Simulated minus observed  $\Delta^{14}\text{C}$  values.

Figures 8, 10, 11, 16, S4, S5, and S6: Lines and dots are blurred.

*There was no option during the original manuscript submission to submit the high resolution PDF figures. These will be uploaded for the production of the final revised paper. In the interim period, we would be happy to supply the editor with a zip file of the original PDFs to be shared with the reviewers. Please let us know what is preferred.*

P 38, Figure 11: The line plots should be replaced with Hovmöller diagrams.

*We will replace the original line plots with Hovmöller diagrams and revise the figure caption, as below:*

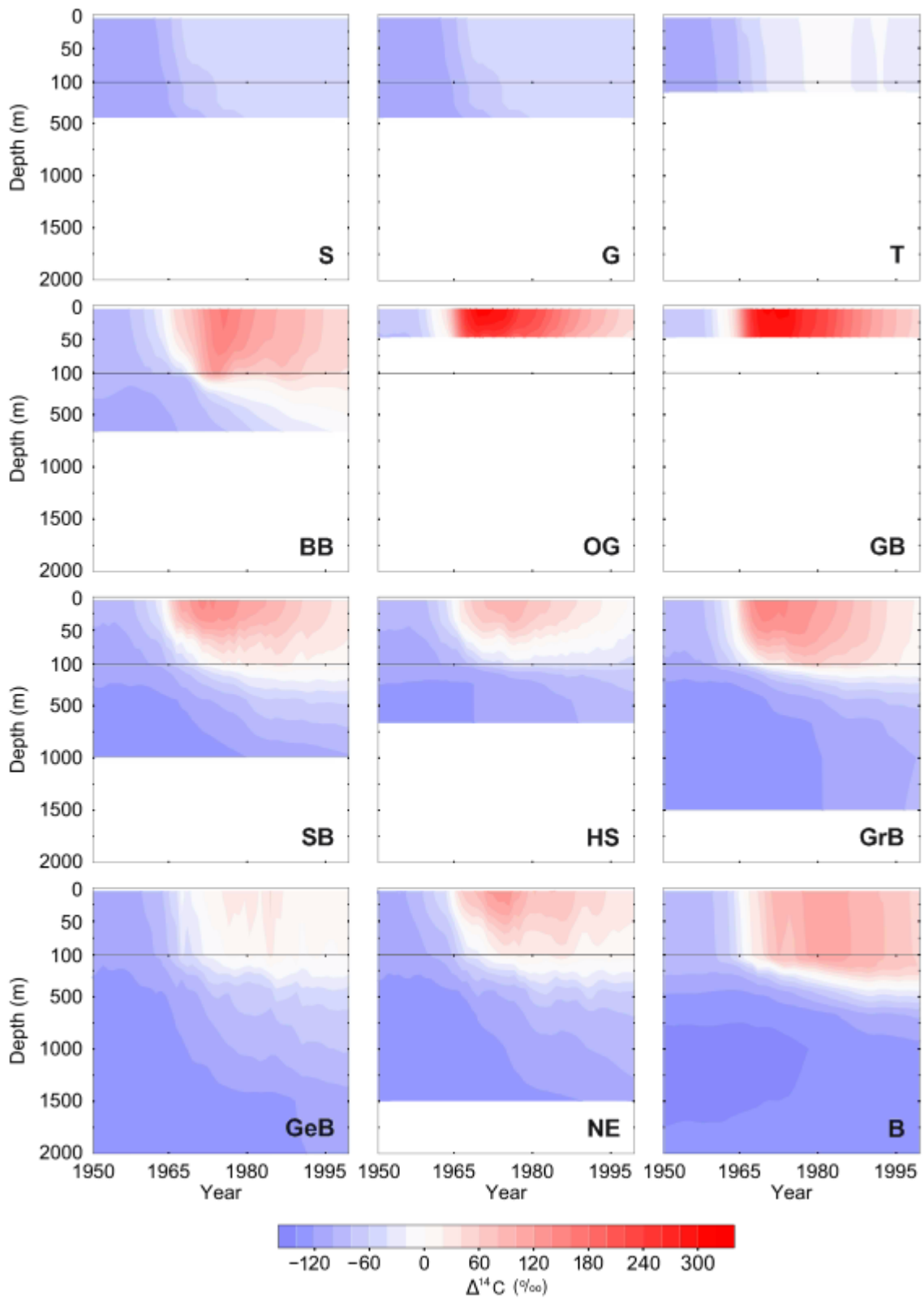


**Figure 11:** Hovmöller diagrams of simulated  $\Delta^{14}\text{C}$  at the coral and bivalve locations (outlined in Figure 9): Bermuda (B), Bay of Biscay (BB), Grimsey (G), German Bight (GB), Georges Bank (GeB), Grand Banks (GrB), Hudson Strait (HS), Northeast Channel (NE), Oyster Ground (OG), Sigrufjörður (S), Sable Bank (SB), and Tromsø (T). Note that the vertical scale has been expanded for the uppermost 100 m of the water column.

SM, P 2: “OCMIP” should read “OCMIP-2”

*This typographical error will be corrected in the revised manuscript.*

## References:

Aumont, O.; Orr, J. C.; Jamous, D.; Monfray, P.; Marti, O.; Madec, G. A Degradation Approach to Accelerate Simulations to Steady-State in a 3-D Tracer Transport Model of the Global Ocean. *Climate Dynamics* 1998, 14 (2), 101–116.

Fiadeiro, M. E. Three-Dimensional Modeling of Tracers in the Deep Pacific Ocean, II. Radiocarbon and the Circulation. *Journal of Marine Research* 1982, 40, 537–550.

Meniel, L.; Yu, J.; Joos, F.; Mouchet, A.; Meissner, K. J.; England, M. H. Poorly Ventilated Deep Ocean at the Last Glacial Maximum Inferred from Carbon Isotopes: A Data-Model Comparison Study. *Paleoceanography* 2017, 32 (1), 2016PA003024.

Mouchet, A. The Ocean Bomb Radiocarbon Inventory Revisited. *Radiocarbon* 2013, 55, 1580–1594.

Orr, J. C.; Najjar, R. G.; Aumont, O.; Bopp, L.; Bullister, J. L.; Danabasoglu, G.; Doney, S. C.; Dunne, J. P.; Dutay, J.-C.; Graven, H.; et al. Biogeochemical Protocols and Diagnostics for the CMIP6 Ocean Model Intercomparison Project (OMIP). *Geosci. Model Dev.* 2017, 10 (6), 2169–2199.

Orr, J. C.; Najjar, R. G.; Aumont, O.; Bopp, L.; Bullister, J. L.; Danabasoglu, G.; Doney, S. C.; Dunne, J. P.; Dutay, J.-C.; Graven, H.; et al. Biogeochemical Protocols and Diagnostics for the CMIP6 Ocean Model Intercomparison Project (OMIP). *Geosci. Model Dev.* 2017, 10 (6), 2169–2199.